JOURNAL OF MAPS
2024, VOL. 20, NO. 1, 2422543
https://doi.org/10.1080/17445647.2024.2422543

Taylor & Francis
Taylor & Francis Group

Science

Geological study of the seafloor applied to marine renewable energies

Iván Asensio[a], Lidia Rodríguez-Méndez[b], Néstor Vegas[b] and Aitor Aranguren[b]

[a]Basque Country University UPV/EHU, Leioa, Spain; [b]Geology Department, Basque Country University UPV/EHU, Leioa, Spain

ABSTRACT

This paper shows an example of how to create morphological and geological maps of the seabed combining high-resolution bathymetric data and onshore geological information. The mapped area corresponds to the BIMEP offshore test site, located in the south-eastern part of the Bay of Biscay, in the northern part of the Iberian Peninsula. In the Morphological map, using semi-automatic methods, the seafloor is categorized in 10 classes, obtained by the combination of terrain variables and a decision table. In the Geological map, onshore-defined geological units are extended into the continental shelf, and bedding traces, folds, and fractures are depicted. These maps could serve as valuable tools for stakeholders involved in marine energy projects, enabling informed decision-making and promoting sustainable development practices.

ARTICLE HISTORY
Received 27 February 2024
Revised 16 September 2024
Accepted 22 October 2024

KEYWORDS
Geological map; Marine geology; Morphobathymetrical map; Basque-Cantabrian Basin; BIMEP

1. Introduction

As the world moves toward a greener future, understanding the seabed's composition and dynamics becomes increasingly vital in facilitating the transition to renewable energy sources. This understanding is fundamental for harnessing the vast potential of marine resources such as offshore wind, tidal, and wave energy. Offshore wind energy, for instance, relies on the geological stability of the seabed to support the installation of wind turbines.

Moreover, the study of the seabed geology extends beyond energy considerations to encompass broader environmental concerns such as conservation, biodiversity protection, and disaster risk management. Understanding geological hazards like submarine landslides, seafloor subsidence, and volcanic activity is essential for safeguarding coastal communities, infrastructure, and ecosystems. By integrating geological insights into strategic planning and decision-making processes, we can unlock the full potential of marine renewable energy resources while preserving the integrity of our oceans for future generations.

Marine energy testing facilities, like BIMEP (Biscay Marine Energy Platform) in the Bay of Biscay, near the Basque Country in Spain, play an essential role in the energy transition toward more sustainable and renewable sources. BIMEP offers a testing ground in real marine conditions for researchers and developers to assess the performance of wave and offshore floating wind energy devices before deploying them on a larger scale. Additionally, they provide a complete characterization of the testing area, including topographical, hydrodynamical, and geophysical studies (Colominas et al., 2013; ESGEMAR, 2017; Galparsoro & Blangy, 2009). In this work, we used some of this information, such as high-resolution bathymetry (Bald, 2017), in order to perform a geological analysis of the seafloor, including a morphological and a geological map. This information could be used to facilitate the identification of optimal locations for future installations and to optimize the management and maintenance of existing ones.

2. Geological background

2.1. Basque-Cantabrian shelf

This study focuses in an area of 16 km^2 of the Basque continental shelf, in the southeastern part of the Bay of Biscay (Figure 1), where the BiMEP test site is placed. The continental shelf in this sector of the Cantabrian Sea is characterized by its narrowness; it varies from 7 km in front of Matxitxako Cape to 20 km in front of the Oria Estuary (Uriarte, 1998). The Cantabrian shelf shows a staircase morphology, with 12 submerged terraces irregularly preserved, that is controlled by an interplay of variables such as wave climatology, lithology, and bedding direction (Bilbao-Lasa et al., 2020).

Oceanographic setting along the Bay of Biscay is related to the North Atlantic low-pressure and Azores

CONTACT Lidia Rodríguez-Méndez lidia.rodriguez@ehu.eus Geology Department, Basque Country University UPV/EHU, B° Sarriena SN, 48940 Leioa, Spain

Supplemental data for this article can be accessed online at https://doi.org/10.1080/17445647.2024.2422543.

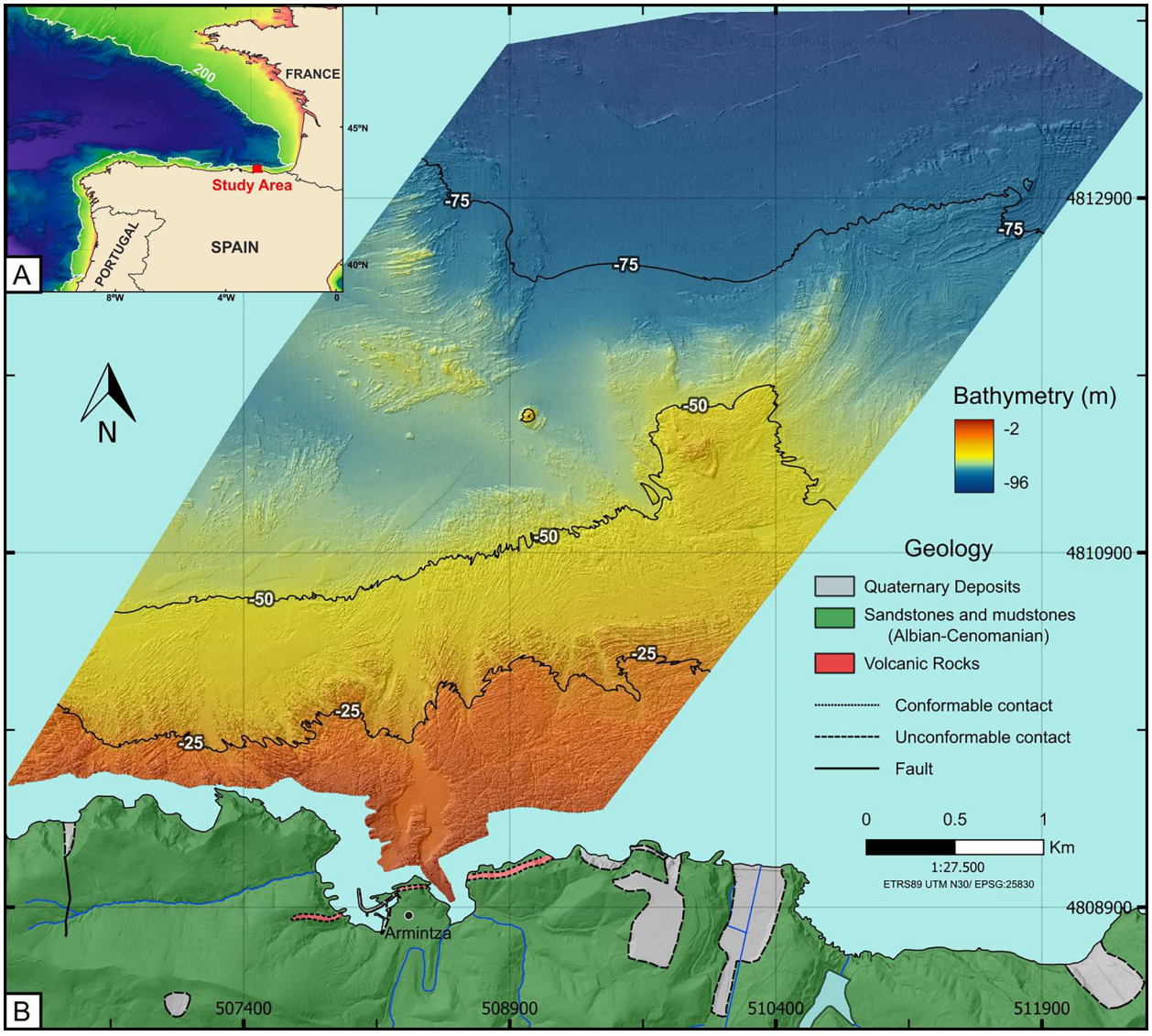

Figure 1. (A) Location of the study area in the north of the Iberian Peninsula. (B) Detailed map of the studied zone, including a simplified onshore geological map and a digital terrain model of the sector of continental shelf hosting the Biscay Marine Energy Platform site (BIMEP).

high-pressure systems (Uriarte et al., 2004). Wind-driven currents are the predominant water circulation cause (Fontán & Cornuelle, 2015; Fontán et al., 2009) and are characterized by strong NW swell waves related to large storms (Galparsoro & Blangy, 2009; Galparsoro et al., 2010; Uriarte et al., 2004). The tidal influence in platform currents is mostly limited to estuaries (Uriarte et al., 2004) mainly because of the narrowness of the continental shelf (Fanjul et al., 1998; Fontán et al., 2009). Referring to sediment supply along the Basque Country continental shelf, the major suppliers are coastal erosion and rivers, $1.57{\cdot}10^6$ t/yr suspended material discharged by 12 main rivers (Ferrer et al., 2009; Uriarte et al., 2004).

2.2. Regional geological setting

The Cantabrian margin shows a complex tectonic evolution as the result of consecutive extensive and compressive tectonic cycles that were initiated in Paleozoic times (Tugend et al., 2014). The studied area is placed in the northern border of the so-called Basque-Cantabrian Basin (BCB), which constitutes the western prolongation of the Pyrenees. The BCB is a hyperextended basin inverted during Cenozoic times due to the Alpine Orogeny (García-Mondéjar et al., 1996; Gómez et al., 2002; Roca et al., 2011), filled by a Mesozoic to Cenozoic sedimentary succession with interlayered Aptian to Santonian basic volcanic rocks (Agirrezabala et al., 2017; Cuevas et al., 1999; García-Mondéjar et al., 2018). This study focuses on the most intensely deformed portion of the BCB, where northeast-vergent thrusts, strike-slip subvertical faults, and major folds crop out (Ábalos, 2016; Cuevas et al., 1999).

The coastal sector close to the study area shows an ENE-trending succession from Albian to Cenomanian times. Previous maps have distinguished the following units (Garrote Ruiz et al., 1987):

- The Monte Grande Formation (Lower-Middle Albian). It crops out in the western part of the study area and is formed by siliceous sandstones and/or conglomerates with laminated siltstones interlayered. Dark colors are commonly observed due to the abundance of plant fossils.
- The Black Flysch Formation (Upper Albian-Lower Cenomanian). Discordantly covers the Monte Grande Formation and is composed by a flysch sequence of alternating layers of sandstones, conglomerates, and shales, where slumps (Figure 2A) and debris flows are often recognized. Under the microscope, sandstones can be more precisely classified as sublitharenites (Folk, 1954) and are formed by subrounded to angular grains of quartz, white micas, and iron oxides, in a fine-grained calcitic matrix. Conglomerates are often polymictic paraconglomerates, composed by polycristalline quartz, rock fragments, and bioclasts in a fine-grained matrix (Figure 2B).
- The Volcanic Complex (Upper Albian, Castañares & Robles, 2004). In the studied area, it is composed by decimetric to decametric levels of vulcanoclastic rocks, pillow lava flows, and massive flows (Figure 2C), interlayered within the Black Flysch formation. Under the microscope, pillow lavas are very weathered and only plagioclases and calcite-filled vacuoles are identified (Figure 2D).

3. Data and methods

The study combines field work, restricted to the coastal area in order to characterize the main lithologies and structures, with the analysis of high-resolution bathymetric data provided by BiMEP. The bathymetric campaign was carried out in September 2017 on board the AZTIMAR BAT (Bald, 2017), equipped with the SeaBat 7125 high-resolution multibeam echosounder (MBES) from the Reson group (RESON, 2006). This MBES operates at 400 kHz, using 256 beams to cover a 128° angular sector, giving a vertical resolution of 6 mm and being able to operate at max depth near 100 m. The final digital elevation models (DEMs) were obtained with a cell size of 1 m.

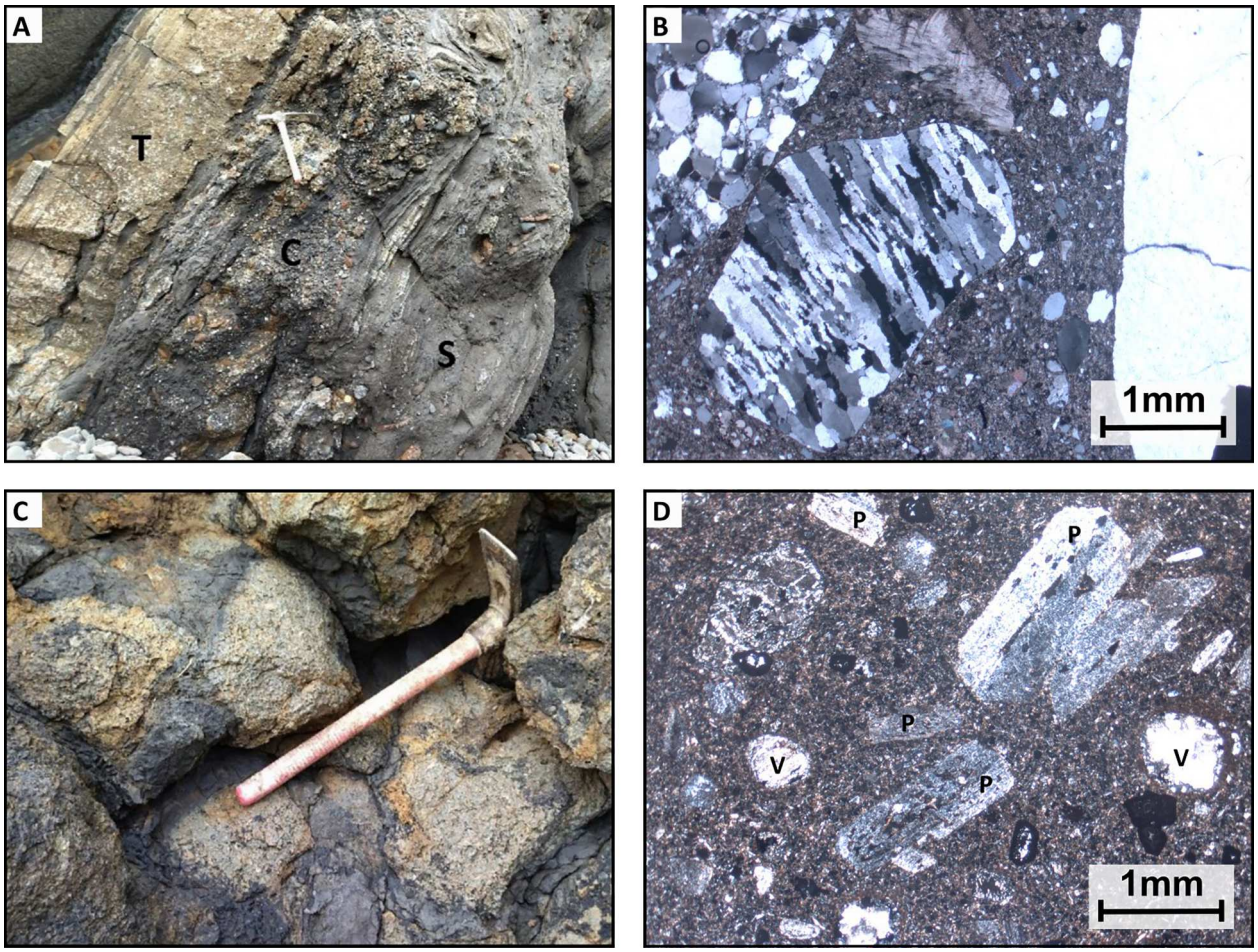

Figure 2. (A) Example of an outcrop of the Black Flysch Formation, composed by yellow colored sandstones of turbiditic origin (T), a conglomeratic bed (C) and a slumped layer (S) at the bottom of the image. (B) Microphotograph of the conglomeratic bed in Figure 2A showing three quartz lithoclasts, millimetric to centimetric in size, and a smaller bioclast in a fine grain matrix mainly composed by quartz grains and calcite. (C) Photograph of a pillow lava flow of the volcanic complex. (D) Microphotography of the pillow lava in Figure 2C showing a holocrystalline, microporphyritic texture with plagioclase crystals (P) and vacuoles (V) in a fine grain matrix.

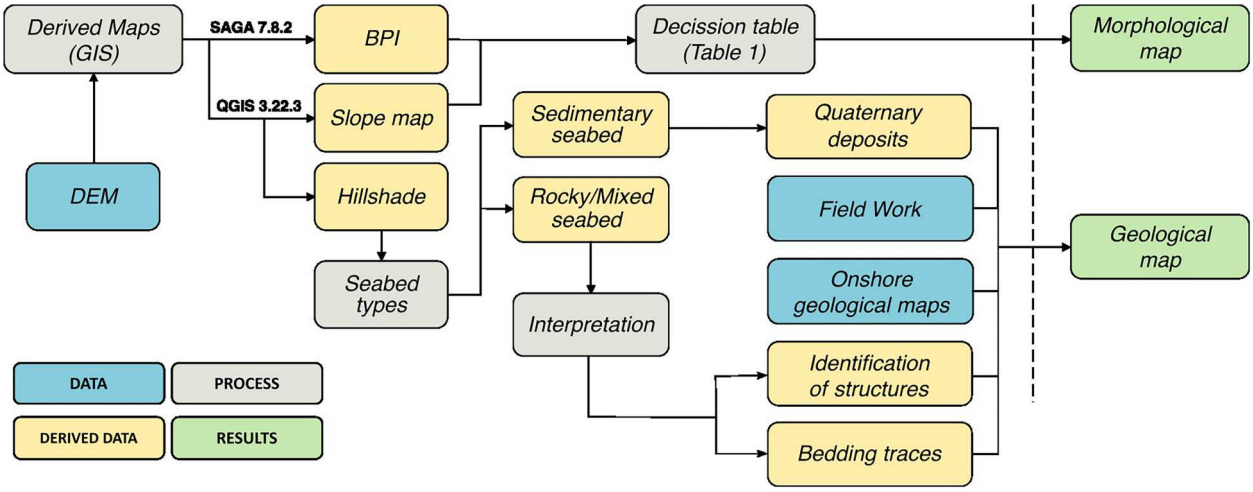

Figure 3. Flow chart summarizing the methodology used during the desk work. The blue boxes correspond to the original data sets, the gray ones are the procedures followed, the yellow ones show the derived data and the green ones show the final deliverables.

In order to manage and process all the data, QGIS 3.22.3 and SAGA 7.8.2 are used (Figure 3). QGIS served as the primary program for loading the bathymetric data and mapping faults, bedding traces, and the extension of the geological units toward the shelf, to create the Geological Map. QGIS also served to correct cells without data using the GDAL library's 'fill nodata module'. The corrected bathymetry is then used to calculate slope, roughness, and hillshade terrain attributes.

The fine and broad bathymetric position indexes (BPI) were calculated using the SAGA module 'Topographic Position Index' under the Terrain Analysis – Morphometry section. Terrain attributes derived from bathymetric data, such as broad- and fine-scale bathymetric position index (BPI), slope, roughness, and hillshade (Lundblad et al., 2006), are used to capture seafloor general morphological characteristics and then to perform the seabed classifications and their respective maps.

4. Morphological map

Using a semi-automatic method, the seafloor is categorized into 10 morphology classes defined by a morphological feature that is obtained by the combination of terrain variables and a decision table (Table 1), modified from Jerosch et al. (2016). These variables are the slope of the seabed (the inclination of the seabed expressed in degrees) and the broad and fine-scale Benthic Positioning Indexes (BPI). BPI measures the difference between a focal cell elevation value and the mean elevation of surrounding cells; different scales of BPI are used to describe fine and broad benthic features. The Broad BPI highlights the major landscape features (e. g. regional depressions), while the Fine BPI captures the fine details (e.g. pinnacles). Moreover, BPI negative values correspond to lower points than surrounding areas (depressions), whereas BPI positive values represent higher points and near-zero values denote constant-slope or flat areas (Lundblad et al., 2006). In order to establish a scale factor that represents better the study area, an analysis of the most relevant morphologies is conducted, finding a fine-scale radius of 0–25 m and a broad scale radius of 10–100 m. To be able to compare each BPI scale, both indexes were normalized by standardizing to 1 standard deviation. Aiming to get simpler values, standardized values were multiplied by 100, getting the −100–100 range shown in the decision table (Wienberg et al., 2013).

The resulting morphological map shows 10 classes, grouped into 3 main categories:

- Positive features: ridge, local ridge, flat top ridge, and pinnacle on slope
- Negative features: depression, local depression, and trough
- Slope features: plain, gentle slope, and steep slope.

Positive and negative features are obtained taking into account Fine and Broad BPI values whereas slope features derive from the analysis of the slope gradient of the bedfloor – plain areas (0°–5°), gentle slopes (5°–15°), and steep slopes (>15°). However, slopes between 0 and 3° are proved to be linked to the inherent noise during data acquisition in the area, so to avoid that problem, the threshold for flat areas is established in 3°–5°.

The morphological map shows that the studied area is mostly flat, where plains represent the 56% of the area. Positive features constitute over the 12% of the map and consist on convex features at the upper part of slopes, connecting slopes with depressions. One of the most relevant seafloor features, a circular promontory of 35 m above the near seafloor (Figure

Table 1. Decision table outlining the criteria for the morphological classification based on the terrain variables broad BPI, fine BPI and slope. Modified from Jerosch et al. (2016).

		Broad scale BPI		Fine-scale BPI		Slope	
ID	Seafloor classification	Lower	Upper	Lower	Upper	Lower	Upper
1	Ridge	100		100			
2	Local ridge	−100	100	100			
3	Flat top ridge	100		−100	100		
4	Pinnacle on slope	100		−100	100	5	
5	Plain	−100	100	−100	100		5
6	Gentle slope	−100	100	−100	100	5	15
7	Steep slope	−100	100	−100	100	15	
8	Depression	−100	100		−100		
9	Local depression		−100	−100	100		
10	Trough		−100		−100		

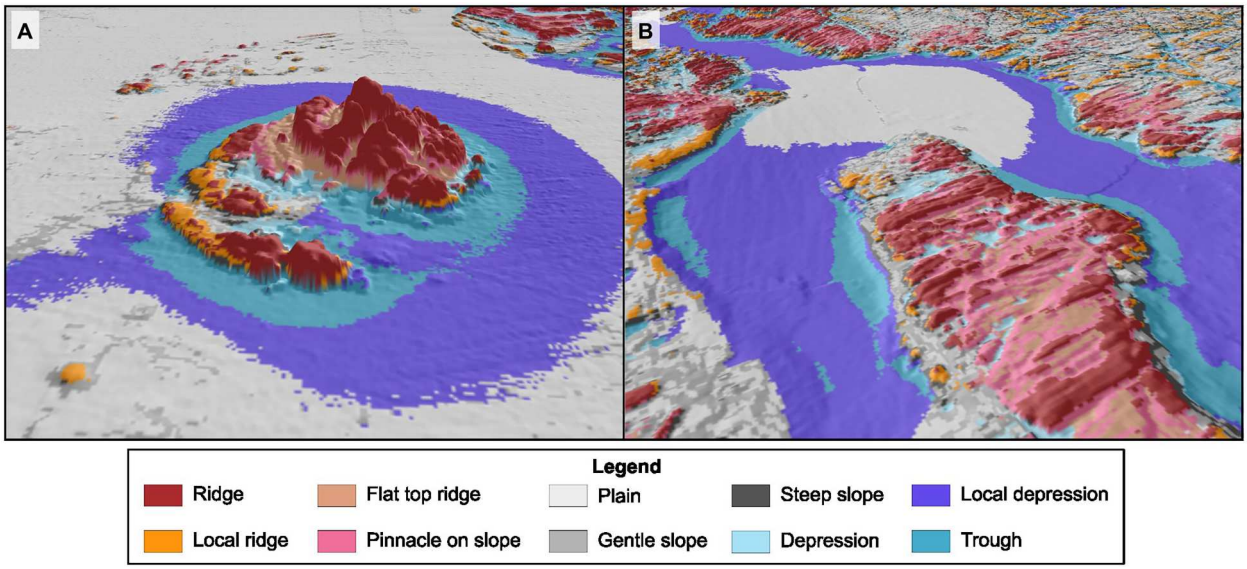

Figure 4. (A) 3D detailed view of the morphological map showing the promontory located in the central zone of the study area. (B) 3D detailed view of the morphological map showing the channel located in the southern sector of BIMEP. The bottom of the image corresponds to the bifurcation of the channel close to the shoreline.

4A), appears in the central zone of the map surrounded by depression and trough classes. Negative features also constitute over the 12% of the study area and are located at the bottom of ridges and/or related to channels. An outstanding feature is the S–N channel observed in the southern sector (Figure 4B), with 2.2 km long, 55–60 m wide covering an area of 0.18 km^2. The channel´s water depth ranges from 13 m at the head to 58 m at the northern end. The cross-sectional profile is asymmetric with walls from 1.5 to 9 m high with slop gradients from 20° to 45°. The longitudinal profile is characterized with plain, depression, local depression, and trough classes, the last ones always appear adjacent to the steep walls.

5. Geological map

Hillshade, both BPI scales, slope, and roughness maps are used to manually build the Geological Map of the studied area at 1:5000 scale. Field data and high-resolution orthophotos of the intertidal area are used in order to complete the area without bathymetrical information and to provide a continuous map from the coastline to the continental shelf.

Five different geological units have been described in the studied area. The unit corresponding to the quaternary materials, formed by unconsolidated sediments, occupies the 39% of the study area and is mainly distributed in the central and the northernmost parts. The rest of the seabed is occupied by rocky bottoms, where bedding traces, faults, and folds are drawn in order to better establish the location of the main geological contacts. Taking into account, Garrote Ruiz et al. (1987) onshore geological map, lithological units (Monte Grande and Black Flysch Formations) are extended into the continental shelf. Nevertheless, the lower contact of the Monte Grande formation does not crop out in the coastal zone, and no other type of information is available to precisely determine its position. Therefore, only an estimated position is shown in the map in order to represent the minimum thickness of the Monte Grande Formation based on regional data (Garrote Ruiz et al., 1987). North of the established lower boundary of

the Monte Grande Formation, the materials are depicted as undifferentiated rocky substrate.

When analysing the layout of the bedding traces mapped in the offshore, the presence of kilometer- to hectometer-scale folds affecting the whole series of materials is evident. Particularly noticeable are the NW–SE oriented folds at the upper right-hand boundary of the geological map. In reference to brittle structures, given the minimal relief of the seabed in the surveyed area, all interpretations have been conducted from a zenithal perspective, making it challenging to identify kinematic criteria for determining fault movement directions. Consequently, no distinction is made between fractures and faults.

6. Discussion and conclusions

In this work, we present a Morphological and a Geological map of the continental shelf from 0 to 96 m depth. A semi-automatic Morphobathymetrical map is generated by the combination of terrain variables and a decision table modified from Jerosch et al. (2016). Ten morphological classes are differentiated and visually represent the main features of the study area. Moreover, bathymetrical analysis coupled with fieldwork in coastal areas allows us to create a Geological map of the continental shelf. Taking into account onshore geological information (Garrote Ruiz et al., 1987), Monte Grande and Black Flysch formations are extended into the shelf. In the case of Monte Grande formation, its lower contact does not crop out onshore, so only a tentative contact is drawn in the shelf in order to represent its minimum thickness based on regional data (Garrote Ruiz et al., 1987). Due to the lack of precise geological information, north to the Monte Grande formation bedrock is depicted as undifferentiated rocky substrate. Lastly, sedimentary covered seabed is represented as undifferentiated quaternary deposits.

There is a direct relation between some of the morphological classes and the geological map. For example, in general, quaternary deposits correspond to plains, depressions, and throughs in the morphological map, whereas rocky substrate is equivalent to positive topographical features and sometimes to gentle and steep slopes. Fracture pattern is well represented by the 'trough' class, especially in the southeastern part of the map. However, this assumption should be made carefully because in the southwestern third the 'trough' class mainly highlights the bedding trace, as it corresponds to the erosion of less competent rocks (e.g. siltstones or shales).

In addition, taking into account the Geological map of the continental shelf and the topographical characteristics of the coast, some of the features recognized in the Morphological map could be geomorphologically interpreted. The clearest example is the channel described in previous sections, located in the central bottom part of the map, as well as two smaller ones east of it. These channels can be interpreted as paleochannels, generated during periods of lower sea levels when rivers extended their courses across the exposed shelf, carving valleys into the sedimentary layers.

In this work, we develop a methodology to generate a Geological and a Morphological map of the continental shelf based on a bathymetrical analysis and onshore geological information. This kind of maps obtained at a relative low cost could constitute the first steps for a more complete geological analysis applied to potential renewable energies sites. Moreover, with this methodology, once the main morphological characteristics of a sector are established, new Morphological maps can easily be created in order to address, for example, the variation of some of the morphologies with time (e. g. related to the mobility of the sediment) or to generate new maps of adjacent sectors. That kind of information could facilitate offshore infrastructure planning and design, as well as reduce maintenance costs.

Software

QGIS 3.22.3 and SAGA 7.8.2 were used to perform morphological and geological analysis. The design of the final map was produced using QGIS with additional refinement using the open-source Inkscape software.

Acknowledgments

We would like to thank BIMEP for providing the bathymetric information. Constructive suggestions from reviewers J. Pánek, P. Lemenkova, and the editor-in-chief M. J. Smith improved the final version of the manuscript. Iván Asensio – conceptualization, conducted the investigation, mapping and data acquisition, fieldwork, methods, analysis and interpretation of results, elaborated figures, and writing. Lidia Rodríguez-Méndez – conceptualization, conducted the investigation, analysis and interpretation of results, writing, review, and supervision. Néstor Vegas – conceptualization, analysis and interpretation of results, elaborated figures, writing, review, and supervision. Aitor Aranguren – analysis and interpretation of the results and review.

Disclosure statement

No potential conflict of interest was reported by the author(s).

Funding

This work was supported by project PID2022-136948NB-100/AEI/10.13039/501100011033/FEDER, UE (Spanish Ministry of Science and Innovation) and project GIU23/003 (University of the Basque Country, UPV/EHU).

Data availability statement

The data that support the findings of this study are available from the corresponding author, L. R-M, upon reasonable request.

References

Ábalos, B. (2016). Geologic map of the Basque-Cantabrian Basin and a new tectonic interpretation of the Basque Arc. *International Journal of Earth Sciences*, *105*(8), 2327–2354. https://doi.org/10.1007/s00531-016-1291-6

Agirrezabala, L., Sarrionandia, F., & Carracedo, M. (2017). Diatreme-forming volcanism in a deep-water faulted basin margin: Lower Cretaceous outcrops from the Basque-Cantabrian Basin, western Pyrenees. *Journal of Volcanology and Geothermal Research*, *337*, 124–139. https://doi.org/10.1016/j.jvolgeores.2017.03.019

Bald, J. (2017). Estudio Batimétrico en BIMEP. Informe para BIMEP, S.A., p. 9.

Bilbao-Lasa, P., Jara-Muñoz, J., Pedoja, K., Alvarez, I., Aranburu, A., Iriarte, E., & Galparsoro Iza, I. (2020). Submerged marine terraces identification and an approach for numerical modeling the sequence formation in the Bay of Biscay (Northeastern Iberian Peninsula). *Frontiers in Earth Science*, *8*, 47. https://doi.org/10.3389/feart.2020.00047

Castañares, L. M., & Robles, S. (2004). El vulcanismo del Albiense-Santoniense en la Cuenca Vasco-Cantábrica. In J. A. Vera (Ed.), *Geología de España* (pp. 306–308). Instituto Geológico y Minero de España - Sociedad Geológica de España.

Colominas, M., Liria, P., & Galparsoro, I. (2013). Campaña batimétrica previa a la instalación de los cables en bimep. Elaborado por AZTI-Tecnalia para Zumaia Offshore, p. 337.

Cuevas, J., Aranguren, A., Badillo, J. M., & Tubia, J. M. (1999). Estudio estructural del sector central del Arco Vasco (Cuenca Vasco-Cantábrica). *Boletin Geologico y Minero*, *1*, 3–18.

ESGEMAR. (2017). Campaña de sísmica de reflexión en el área de BIMEP, Armintza (Vizcaya). Informe de resultados para Biscay Marine Energy Platform S.A., p. 31.

Fanjul, E. A., Gomez, B. P., Carretero, J. C., & Arevalo, I. R. S. (1998). Tide and surge dynamics along the Iberian Atlantic coast. *Oceanologica Acta*, *21*(2), 131–143. https://doi.org/10.1016/S0399-1784(98)80003-0

Ferrer, L., Fontán, A., Mader, J., Chust, G., González, M., Valencia, V., Uriarte, A., & Collins, M. B. (2009). Low-salinity plumes in the oceanic region of the Basque Country. *Continental Shelf Research*, *29*(8), 970–984. https://doi.org/10.1016/j.csr.2008.12.014

Folk, R. L. (1954). The distinction between grain size and mineral composition in sedimentary-rock nomenclature. *The Journal of Geology*, *62*(4), 344–359. https://doi.org/10.1086/626171

Fontán, A., & Cornuelle, B. (2015). Anisotropic response of surface circulation to wind forcing, as inferred from high-frequency radar currents in the southeastern Bay of Biscay. *Journal of Geophysical Research: Oceans*, *120*(4), 2945–2957. https://doi.org/10.1002/2014JC010671

Fontán, A., Manuel, G., Wells, N., Collins, M., Mader, J., Ferrer, L., Esnaola, G., & Uriarte, A. (2009). Tidal and wind-induced circulation within the Southeastern limit of the Bay of Biscay: Pasaia Bay, Basque Coast. *Continental Shelf Research*, *29*(8), 998–1007. https://doi.org/10.1016/j.csr.2008.12.013

Galparsoro, I., & Blangy, A. (2009). Estudio geofísico en la zona de BiMEP (Arminza). Elaborado por AZTI-Tecnalia para Robotiker-Tecnalia, 31, + planos.

Galparsoro, I., Borja, A., Legorburu, I., Hernández, C., Chust, G., Liria, P., & Uriarte, A. (2010). Morphological characteristics of the Basque continental shelf (Bay of Biscay, northern Spain); their implications for Integrated Coastal Zone Management. *Geomorphology*, *118*(3-4), 314–329. https://doi.org/10.1016/j.geomorph.2010.01.012

García-Mondéjar, J., Agirrezabala, L. M., Aranburu, A., Fernández-Mendiola, P. A., Gómez-Pérez, I., López-Horgue, M., & Rosales, I. (1996). Aptian— Albian tectonic pattern of the Basque— Cantabrian Basin (Northern Spain). *Geological Journal*, *31*(1), 13–45. https://doi.org/10.1002/(SICI)1099-1034(199603)31:1<13::AID-GJ689>3.0.CO;2-Y

García-Mondéjar, J., Carracedo, M., Owen, H., & Fernandez-Mendiola, K. (2018). The Early Aptian volcanic episode of Gutiolo (N Spain): Expression of the Bilbao Rift Fault Zone. *Geological Journal*, *54*(6), 3509–3526. https://doi.org/10.1002/gj.3342

Garrote Ruiz, A., García Portero, J., Muñoz Jiménez, L., Arriola Garrido, A., Eguiguren Altuna, E., García Pascual, I., & Garrote Ruiz, R. (1987). Memoria y mapa geológico a escala 1:25.000 de la hoja n° 37 (Armintza). EVE.

Gómez, M., Vergés, J., & Riaza, C. (2002). Inversion tectonics of the Northern margin of the Basque Cantabrian Basin. *Bulletin de la Société Géologique de France*, *173*(5), 449–459. https://doi.org/10.2113/173.5.449

Jerosch, K., Kuhn, G., Krajnik, I., Scharf, F. K., & Dorschel, B. (2016). A geomorphological seabed classification for the Weddell Sea, Antarctica. *Marine Geophysical Research*, *37*(2), 127–141. https://doi.org/10.1007/s11001-015-9256-x

Lundblad, E. R., Wright, D. J., Miller, J., Larkin, E. M., Rinehart, R., Naar, D. F., Donahue, B. T., Anderson, S. M., & Battista, T. (2006). A Benthic Terrain Classification Scheme for American Samoa. *Marine Geodesy*, *29*(2), 89–111. https://doi.org/10.1080/01490410600738021

RESON. (2006). SeaBat 7125 Operator´s manual, v. Version 3.0, p. 89.

Roca, E., Muñoz, J., Ferrer, O., & Ellouz, N. (2011). The role of the Bay of Biscay Mesozoic extensional structure in the configuration of the Pyrenean orogen: Constraints from the MARCONI deep seismic reflection survey. *Tectonics*, *30*(2), 1–33. https://doi.org/10.1029/2010TC002735.

Tugend, J., Manatschal, G., Kusznir, N. J., Masini, E., Mohn, G., & Thinon, I. (2014). Formation and deformation of hyperextended rift systems: Insights from rift domain mapping in the Bay of Biscay-Pyrenees. *Tectonics*, *33*(7), 1239–1276. https://doi.org/10.1002/2014TC003529

Uriarte, A. (1998). *Sediment dynamics on the inner continental shelf of the Basque Country (N.Spain)* [Doctoral dissertation]. University of Southampton.

Uriarte, A., Collins, M., Cearreta, A., Bald, J., & Evans, G. (2004). Sediment supply, transport and deposition: Contemporary and Late Quaternary evolution. In Á. Borja & M. Collins (Eds.), *Oceanography and Marine Environment of the Basque Country* (Vol. 70, pp. 97–132). Elsevier Oceanography Series.

Wienberg, C., Wintersteller, P., Beuck, L., & Hebbeln, D. (2013). Coral Patch seamount (NE Atlantic) – A sedimentological and megafaunal reconnaissance based on video and hydroacoustic surveys. *Biogeosciences*, *10*(5), 3421–3443. https://doi.org/10.5194/bg-10-3421-2013